Soft Matter

Accepted Manuscript

ROYAL SOCIETY OF CHEMISTRY

www.rsc.org/softmatter

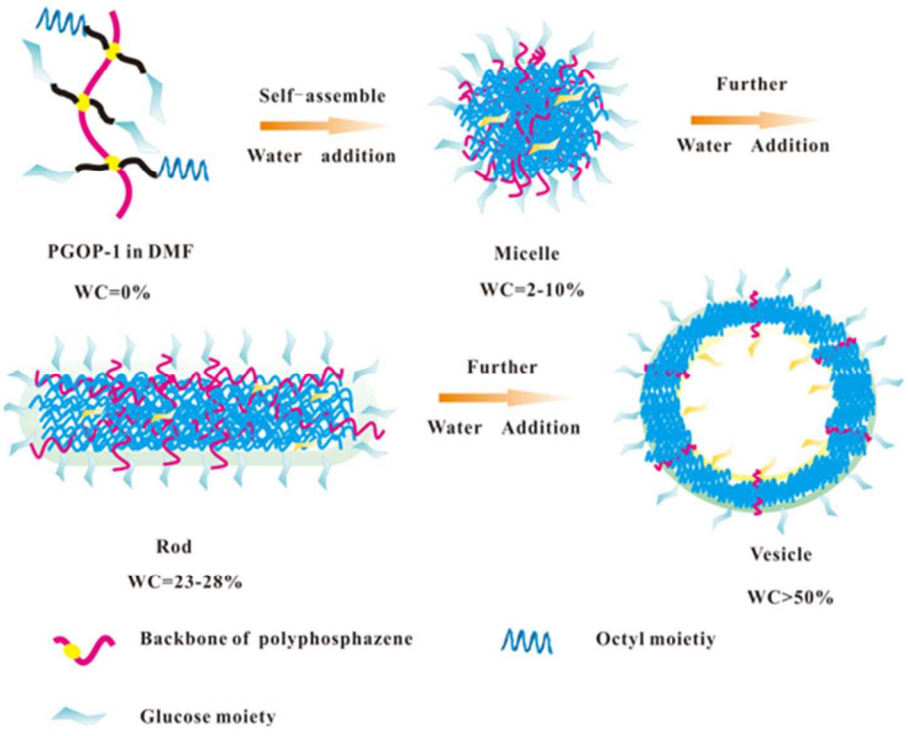

Table of contents

173x157mm (96 x 96 DPI)

[Prepared as a full paper for Publication in ***Soft Matter***]

Self-assembly and Morphological Transitions of Random Amphiphilic Poly(*β*-D-glucose-*Co*-1-octyl) phosphazenes

Chen Chen[1]; Yue-Cheng Qian[1]; Chuan-bin Sun[2]; Xiao-Jun Huang[1]

[1] MOE Key Laboratory of Macromolecular Synthesis and Functionalization, Department of Polymer Science and Engineering, Zhejiang University, Hangzhou 310027, China

[2] Eye Center, Second Affiliated Hospital of Zhejiang University School of Medicine, Hangzhou, 310009, China

Correspondence to: X. J. Huang (E-mail: hxjzxh@zju.edu.cn)

Abstract

The amphiphilic random copolymer poly(*β*-D-glucose-*Co*-1-octyl)phosphazene (PGOP) can undergo continuous morphological transitions in DMF-water mixed solvents. In this study, the ratio of glucose moieties to octyl moieties was controlled via a two-step thiol-ene reaction. As a result, polyphosphazenes with glycosyl functionalization degrees of 58.1% (PGOP-1), 74.1% (PGOP-2) and 87.0% (PGOP-3) were obtained. These amphiphilic polyphosphazenes self-assemble in both water and water-DMF mixtures. Several self-assembled morphologies including spheres, rods and vesicles were formed though careful control of the water content (WC) in the DMF solvent as well as of the hydrophilicity or hydrophobicity of the copolymers. We also found that increases in the hydrophobic proportion led to faster morphological transitions at a constant WC. The thermodynamics of micellization were also studied by Isothermal Titration Calorimetry (ITC), and the strong hydrophobic interactions in PGOP-1 were demonstrated by their highly exothermic nature. These self-assemblies have potential applications in biosensors, lectin adsorption and drug loading with controlled release.

Keywords: Self-assemble; random copolymer; morphological transition

1. Introduction

Block copolymers have been shown to form a wide range of well-organized nano-structures such as spheres, rods, vesicles, large compound micelles (LCM) and other lamellar aggregates[1-8]. The main issue pointed to morphological transition of self-assemblies could be related to the change in interfacial free energy under different temperature, solvent composition, polymer concentration and pH, among other factors[9-13]. Amphiphilic random copolymers share the ability to self-assemble with block copolymers. Firstly, The initial driving force for self-aggregation can be noncovalent interactions including hydrophobic interactions, hydrogen bonding, π-π interactions, coordination, charge-transfer interactions and host-guest inclusion complexation[14-19]. Moreover, through careful molecular design, random amphiphilic copolymers can be induced to form multiple organized self-assemblies, which can be regulated via the balance between hydrophilicity/hydrophobicity and solvent composition[20,21]. However, since the functional groups in random amphiphilic copolymers are randomly distributed along the polymer backbone, the mechanism of self-assembly is quite different from that in block copolymers. Self-assembly by random copolymers has attracted attention due to the simplicity of their synthesis and the common features such as stimuli responsive properties and versatile morphologies for polymeric self assemblies[22,23]. In this contribution, micellar systems originating from random amphiphilic copolymers have numerous potential applications in areas such as micro-reactors, microcapsules, drug delivery systems and encapsulation of various types of guest molecules[24-28].

Polyphosphazenes are a class of organic-inorganic hybrid polymers which possess a backbone

consisting alternating nitrogen and phosphorus atoms with organic or inorganic groups on each side of each phosphorus atom[29-31]. Polyphosphazenes with phenyl, alkyl, hydroxyl, carboxyl, sulfonyl and glucosyl moieties could be obtained via nucleophilic substitution and other post functional methods[32-36]. Recently, the combination between polyphosphazene modification and thiol-ene reaction, which allows for the preparation of well-defined materials with few structural limitations and synthetic requirements[37], not only greatly enhances reaction efficiency, but also leads to polyphosphazene with controlled functional degree[38]. In this case, vinyl polyphosphazene played a role as the precursor in which C=C bonds converted to other functional groups. The whole synthetic process was carried out under mild condition and heavy metal free. Moreover, amphiphilic polyphosphazenes with controlled functionality have the potential for numerous applications in the fields of tissue engineering, drug loading, biosensors and gene delivery[39-46]. Polyphosphazene-based amphiphilic polymers bearing both hydrophobic and hydrophilic moieties can also self-assemble under various conditions with controlled solubility and biocompatibility[47,48].

Due to these features of polyphosphazenes, self-assembly of these amphiphilic polymers has also been explored by a number of reseachers. Zheng et al.[49] designed a pH-responsive polyphosphazene, which was prepared by linking N,N-diisopropylethylenediamine (DPA) onto a backbone of PEGylated polyphosphazene, for cytoplasmic release of doxorubicin in Dox-resistant tumor cells. Tian et al.[50] constructed palm-tree-like self-assemblies based on noncovalent “host-guest” interactions between a phosphazene polymer chain with a terminal adamantyl group and a tetra-branched β-CD-functionalized organic polymeric block. One of the futher potential area of polymeric self-assemblies could possibly be morphological transitions,

which strongly affect properties related to medicine delivery, electronic properties, pollution control and separation[21]. The ability to alter the shapes of phosphazene self-assemblies through variations in solvent composition and the hydrophilicity or hydrophobicity of the polymer could combine the properties of polyphosphazene with interfacial properties of self-assemblies.

In our previous work[51,52], amphiphilic polyphosphazenes with different chemical proportion were synthesized via a two step thiol-ene reaction. Micelles were obtained in aqueous solution through self-assembling process. Moreover, morphological transition took place when water content (WC) increased in water-DMF mixed solution. We came to realize that the morphology of self-assemblies form by random polyphosphazenes could be altered and controlled under certain conditions. Further work was carried out to give insights into this complicated morphological transition triggered by different factors. Thus, poly(*β*-D-glucose-*Co*-1-octyl)phosphazenes (PGOPs) with controlled glucosyl densities, 58.1% (PGOP-1), 74.1% (PGOP-2) and 87.0% (PGOP-3), were obtained, and were shown to self-assemble in both aqueous and DMF-water solutions. Moreover, morphological transitions from micelles to vesicles were monitored by Static Light Scattering (SLS) and Transmission Electron Microscopy (TEM). The results of Dynamic Light Scattering (DLS) demonstrated size expansion from a few hundred nanometers to micrometers as water content increased. Isothermal Titration Calorimetry (ITC) was carried out to measure the thermodynamics of micellization process. These nanoparticles may have potential applications as microreactors, microcontainers and drug delivery systems due to the biocompatibility of polyphosphazenes[53, 54].

2. Experimental Section

2.1. Materials

Hexachlorocyclotriphosphazene (Bo Yuan New Materials & Technique, Ningbo, China) was purified by recrystallization from heptane and subsequent vacuum sublimation at 60 °C. Poly(dichlorophosphazene) was synthesized via thermal ring-opening polymerization of the purified hexachlorocyclotriphosphazene in an evacuated Pyrex tube at 250 °C. The polymer was treated with petroleum ether (Sinopharm Chemical Reagent, China) under a dry nitrogen atmosphere to remove unpolymerized hexachlorocyclotriphosphazene before use. Allylamine (Zoupin Mingxing Chemical Co., China) was purified by vacuum distillation. Tetrahydrofuran (THF) was dried by refluxing over a Na-K alloy in the presence of benzophenone until a blue color was obvious, followed by distillation. Triethylamine (TEA) was dried over CaH_2 prior to use. 2,2-Dimethoxy-2-phenylacetophenone (DMPA, Aladdin Reagent, China), trifluoroethanol (TFE, Aladdin Reagent, China, 99.5%), and 1-octanethiol were used without further purification. 2,3,4,6-Tetra-O-acetyl-1-thiol-*β*-D-glucopyranose (SH-$GlcAc_4$) was synthesized as previously reported.

2.2. Synthesis of Poly[bis(allylamino)phosphazene] (PBAAP)

Poly(dichlorophosphazene) (2.00 g, 17.3 mmol) was dissolved in dry THF (250 mL) and the resulting solution was added in a drop-wise manner to a stirred solution of allylamine (5.2 mL, 69.6 mmol) and TEA (9.7 mL, 69.6 mmol) in dry THF (50 mL) under nitrogen. The mixture was stirred at 25 °C for 24 h and then heated to 40 °C and stirred for a further 18 h at that temperature. The mixture was filtered to remove the resulting triethylamine hydrochloride and

the filtrate was concentrated by evaporation. The concentrated solution was added in a drop-wise manner to an excess of ethanol–water (1:1 by volume) to precipitate the polymer. The solid was subsequently filtered and the filter-cake washed several times with ethanol and dried under a vacuum to give the desired polymer product as a white fibrous solid (1.63 g, 60 %).

2.3. Synthesis of poly(β-D-glucose-co-allylamine)phosphazenes

PBAAP (150mg) was dissolved in TFE at a concentration of 15 mg/mL and the mixture was then transferred to a quartz reactor. SH-$GlcAc_4$ (2 equiv. with respect to the double bonds) and DMPA (0.1 or 0.02 equiv. with respect to the double bonds) were added sequentially to the reactor and N_2 was then gently bubbled through the mixture for 10 min to eliminate dissolved oxygen. The thiol-ene reaction was initiated by UV irradiation (max=365 nm, 0.6 mW/cm^2) and conducted for the described time (40 min, 2 h and 4 h) with stirring at ambient temperature. After the first click reaction, the acetyl protecting group was removed by the addition of a 1 M solution of CH_3ONa in CH_3OH to the polymer solution. The mixture was dialyzed against water for 2 days (molecular weight cut-off: 3.5 kDa) then water was removed by freeze drying process. The ratios of glucose moieties to available allylamine were calculated by comparison of the integrations for the signals at 3.66 ppm and 5.90 ppm in the ^1H NMR spectra.

2.4. Synthesis of poly(β-D-glucose-co-1-octyl)phosphazenes

Glycosylated polyphosphazenes were dissolved in DMF (10mg/mL) and 1-octanethiol (5 equiv. with respect to the double bonds) and DMPA (0.01 equiv.) were added to the solution. The mixture was irradiated under UV light for 1 h and subsequently dialyzed against alcohol for

2 days and water for 1 day, then the final product was obtained by freeze-drying. Three amphiphilic polyphosphazenes with different proportions of glucose moieties, 58.1% (PGOP-1), 74.1% (PGOP-2) and 87.0% (PGOP-3), were prepared. The yield for PGOP was 84.3% for PGOP-1, 81.6% for PGOP-2 and 82.2% for PGOP-3.

2.5. Self-assembly of Poly(β-D-glucose-co-1-octyl)phosphazenes

For self-assembly in aqueous solution, PGOP-1, PGOP-2 and PGOP-3 were directly dissolved in deionized water (18.2 MΩ·cm) to give a final concentration of 0.5mg/mL. The solutions were then sonicated for 15min.

For self-assembly in DMF-water mixtures, poly(*β*-D-glucose-*co*-1-octyl)phosphazenes (PGOP-1, PGOP-2 and PGOP-3) were first dissolved in DMF (0.2 mg/mL), then deionized water was gradually added at a constant rate (1wt %/min) at room temperature with moderate stirring. The morphology of the micelles was quenched by adding a large amount of water after reaching the desired water content. DMF was removed by dialysis against water (molecular weight cut-off: 3.5 kDa).

2.6. Characterization

^{1}H and ^{31}P NMR spectra were recorded on a Bruker Advance DMX500. A 2-5 wt % polymer solution was prepared in DMSO-d_6 for ^{1}H NMR analysis. H_3PO_4 in D_2O was used as an external reference for the ^{31}P NMR measurements. Number-average and weight-average molecular weights and molecular weight distributions were determined using gel permeation chromatography (GPC) by Waters 1525/1414. DMF was used as eluent at a flow rate 1.0 mL min^{-1} at 35°C, with PMMA standards. The solutions of amphiphilic polyphosphazenes (PGOP-1,

PGOP-2 and PGOP-3) were prepared in a similar manner to the crew-cut method. Deionized water was gradually added to DMF solution of PGOP (0.2 mg/mL) with a speed of (1wt %/min) at room temperature with moderate stirring. No filtration was carried out before dynamic light scattering (DLS) measurements. A 90 plus DLS instrument (Brookhaven Germany) was employed to measure the hydrodynamic diameter. Transmission electron microscopy (TEM) was used to observe the microstructures of the self-assembled polyphosphazenes and was performed on a JEM-1200EX (NEC, Japan) microscope with an accelerating rate of up to 120 kV. The Static Light Scattering measurements (SLS) were performed by decreasing the temperature and monitoring the scattered light intensity at a 90° scattering angle. For each measurement, the solutions were allowed to sit at a given temperature for 40 min to ensure that the solutions had reached equilibrium. Isothermal Titration Calorimetry (ITC) experiments were carried out using a TAM III (TA USA). All titrations were performed in DMF with addition of pure water at 25 °C. The reaction cell (V=1 mL) was filled with amphiphilic polyphosphazene (PGOP-1, PGOP-2 or PGOP-3) dissolved in DMF (0.2mg/mL). The computer-controlled 300 μL microsyringe performed 40 injections of 4 μL of pure water at intervals of 10 min into the DMF solution with stirring (100 rpm) at 25 °C. The raw experimental data were reported as the amount of heat produced by each injection of the ligand as a function of time. The amount of heat produced per injection was calculated by the instrument software by integrating the areas under the individual peaks.

--Scheme 1--

3. Results and Discussion

3.1 Synthesis of Poly(β-D-glucose-co-1-octyl)phosphazenes

--Scheme 2-- --Table 1--

As illustrated by Scheme 2, PDCP underwent a nucleophilic reaction with allylamine to replace all of the chloride atoms along the alternating nitrogen-phosphorus backbone. Consequently, poly[bis(allylamino)phosphazene] (PBAAP) was synthesized. ^{31}P NMR (Figure S1 and Figure S2) confirmed that there was no trace of chloride in PBAAP since the peak at 19.9 ppm corresponding to the P-Cl bond was absent. Moreover, the resistance of the allyl moieties to polymerization and intramolecular cyclization make PBAAP a highly suitable precursor to multifunctional polyphosphazene derivatives.

The first step in the functionalization of PBAAP was the introduction of glucose moieties. In this case, 2,3,4,6-tetra-O-acetyl-1-thiol-*β*-D-glucopyranose (SH-GlcAc$_4$) could be quantitatively added to PBAAP using click chemistry through careful control of reaction time to give glycolated polyphosphazenes. As more and more glucose was introduced along the backbone, steric repulsion played a crucial role in the reaction rate. As shown in Figure S3, new multiplets from 3.66 ppm to 5.90 ppm in the ^{1}H NMR were assignable to hydrogen atoms of the glucose moieties. The signals at 4.97–5.17 ppm and 5.85–5.92 ppm were ascribed to the protons of the residual C=C double bonds. Thus, the chemical composition of the copolymers could be calculated accurately from the ^{1}H NMR data by comparing the intensities of the peaks due to the hydrogen in the sugar ring at 3.68 ppm (position 8 in Fig. S3) and the hydrogen belonging to the vinyl group at 5.80 ppm (position 17 in Fig. S3 and Fig. S4). The formula for this calculation is as follows:

$$Glu\% = S_8/(S_8+S_{17})$$

Where Glu% represents the ratio of glucose moieties to available double bonds.

Once confirmed the chemical compositions of the glycosylated PBAAPs, the second thiol-ene step was performed. The reaction rates for the alkyl thiol were consistently faster than those for the thiol with the sterically larger glucose group. The residual vinyl groups were completely consumed after UV irradiation for 1h. The hydrophobic nature of the octyl groups rendered the ultimate polymer amphiphilic. As seen in Figure 1, the peak for the vinyl protons vanished (the gray section in Figure 1 and Figure S4), which suggested complete conversion of C=C bonds into aliphatic groups. Characteristic peaks pointed to the octyl groups (the blue section in Figure 1) including at 0.84 ppm [$CH_2CH_2(CH_2)_5CH_3$], 1.24 ppm [$CH_2CH_2(CH_2)_5CH_3$], 1.60 ppm [$CH_2CH_2(CH_2)_5CH_3$] and 2.47 ppm [$CH_2CH_2(CH_2)_5CH_3$] also appeared. Poly(*β*-D-glucose-*co*-1-octyl)phosphazene could be dissolved in some polar solvents such as water, DMF, DMAC and DMSO.

--Figure 1--

3.2 Self-assembly of Poly(β-D-glucose-co-1-octyl)phosphazenes in water

PBAAP is a highly versatile platform for the preparation of functionalized polyphosphazenes with mutable physicochemical properties via thiol-ene click reactions. Poly(*β*-D-glucose-*Co*-1-octyl)phosphazenes with controlled ratios of glucosyl to octyl moieties prepared using this platform presented different self-assembly behaviors. Wei et al. claimed that the sizes of self-organized nano-objects in water are significantly dependent on molecular

weights, chemical compositions and number of aggregation[55]. Owing to the hydrophilicity of the glucose moieties, the poly(*β*-D-glucose-*Co*-1-octyl)phosphazenes could be directly dissolved in water. The mean hydrodynamic diameters of PGOP-1, PGOP-2 and PGOP-3 were measured by Dynamic Light Scattering (DLS)-ranged from 140nm to 80nm with relatively broad size dispersities (PDI=0.42-0.73). As shown in Figure 2, the sizes were 143 nm for PGOP-1, 102 nm for PGOP-2 and 79 nm for PGOP-3. It could be concluded that the more hydrophobic groups, the bigger the size of the micelle would be. Global micelles could be observed by Transmission Electron Microscopy (TEM) as shown in Figure 3. Although the sizes of these nanoparticles were similar to those measured by DLS, it should be noted that the broad size dispersions still existed since the molecular weight distribution was close to 1.6 for the poly(*β*-D-glucose-*co*-1-octyl)phosphazenes. Variations in functionality between polymer chains also contributed this phenomenon.

--Figure 2-- --Figure 3--

3.3 Self-assembly of Poly(β-D-glucose-co-1-octyl)phosphazenes in DMF/water mixed solvents

Self-assemblies that can vary their morphologies in response to external stimulus are attractive for drug encapsulation, circulation, and targeted release as the properties of these nanoparticles will change when changing from one shape to another. In the case of random copolymers, consecutive morphological transitions are not common. However, proteins with randomly sequenced hydrophilic and hydrophobic amino acids in the linear chain often self-organize to form stable complex morphologies[22]. Herein, micellization was carried out

under a relatively slow nanoscale phase separation via a method similar to that used by Eisenberg et al. for preparing ”crew-cut” micelles[2]. In this experiment, PGOP-1, PGOP-2 and PGOP-3 were first dissolved in DMF and then an appropriate amount of water was added to the solution. The whole process of mophological transitions can be seen in Scheme 1.

--Figure 4--

At the beginning of water addition, the water content (WC) was not sufficient to induce precipitation of hydrophobic parts belonging to polymeric chains. As reflected by Figure 4, once WC reached a critical value, the light scattering intensity rose suddenly, which signified micelle formation and the colloidal character induced by nanophase separation. This turning point for micellization was defined as the critical water content (CWC). PGOP-1, PGOP-2 and PGOP-3 had CWC values of 2.0%, 3.0% and 4.3%, respectively. Therefore, the more hydrophobic ratio the polymer has, the less water was needed to trigger self-aggregation of the polymeric chains. The samples corresponding to the circled points in Figure 4 were viewed by TEM. As demonstrated by Table 2, global micelles ranging in size from 70nm to 200nm were formed when the water content was at or close to the corresponding CWC. Size expansion to larger spheres observed by DLS coexisted with the appearance of the first platform in SLS curve corresponding to SLS as indicated by Figure 4 and Figure 5. The TEM images from Table 2 also showed that the spherical nanoparticles grew bigger with increasing WC while the sizes ranging from 200nm-400nm.

Further addition of water caused a morphological transition from spheres to rods. As illustrated by Figure 4, the second platform showed up as a new phase region for rod. This transition

could be ascribed to increasing surface tension between the spherical hydrophobic core and the solvent. As the sizes of the micelles increased, rods with a lower interfacial energy became a more stable morphology than spheres. Interestingly, the rods appeared to grow with both increased WC and prolongation of the standing time. A possible mechanism for this growth may be the insertion of polymer chains into the already existing self-assemblies, in which rods played the role as moulds. Moreover, due to the dispersity of functionalization ratios among the random copolymer chains, precipitation of individual chains from the mixed solvent and their incorporation into self-assemblies occurred progressively throughout the water-addition process. Thus, the rods formed by poly(*β*-D-glucose-*co*-1-octyl)phosphazene grew in a vertical fashion.

Vesicles were observed only in the case of PGOP-1 under high WC (up to 50%). Considering the absence of the third platform, WC from 30% to 50% was a metastable state region, in which long rods coexist with vesicles. As indicated by Table 2, fusion among vesicles was common and the size distribution was broad. It is likely that both hydrophobic alkyl regions and the hydroxyl groups of the glucose moieties play roles in connecting neighboring vesicles. Since this process effectively reduces the surface area and increases the hydrophilic glucose density on the vesicle surfaces, the vesicles after fusion tended to be more stable with increasing WC.

--Table 2-- --Figure 5--

The results shown in Figure 4 also demonstrated that the more hydrophobic the polymer was, the faster the morphological transitions would be. For the large micelle stage, the WC ranges

were 6%-10% for PGOP-1, 9%-16% for PGOP-2 and 14%-26% for PGOP-3. For the rod stage the WC ranges were 23%-28% for PGOP-1 and 35%-45% for PGOP-2. Vesicles were only observed in PGOP-1 when WC reached 50%. The best explanation for this phenomenon is that increasing hydrophobic proportion in poly(*β*-D-glucose-*Co*-1-octyl)phosphazenes results in greater interfacial tension between the self-assemblies and aqueous solvents. Even though there were no obvious demarcation lines between hydrophilic and hydrophobic regions, the polymeric chains still had the ability to rearrange themselves into different morphologies through hydrophobic interactions and hydrogen bonding. Overall, we can control the morphologies of self-assemblies in different solvent compositions through varying the hydrophilicities and hydrophobicities of the polymers.

--Figure 6--

Isothermal Titration Calorimetry (ITC) was also employed to study the thermodynamics of the micellization process at low WC. In this case, an important factor that must be taken into account in these measurements is the exothermal effect of adding water to DMF. A possible explanation for this is that the hydrogen bonding structures in DMF-water mixtures are stronger than those in pure water[56]. To obtain the heat of micellization (ΔH_{mic}), the heat of solvent mixation (ΔH_{mix}) must be deducted from the observed heat (ΔH_{obs}).

$$\Delta H_{obs} = \Delta H_{mic} + \Delta H_{mix}$$

As demonstrated by Figures 6A, 6C and 6E, each injection of 4 μL water into 800 μL DMF generated 700-800 mJ heat in the absence of an amphiphilic polyphosphazene. ΔH_{mix} increased at the beginning of the water addition process, reached a peak at 5% WC, then

decreased through the rest of the titration process. This phenomenon could be ascribed to variations in the hydrogen bonding structures of DMF-water mixtures. In the initial stage of the titration, each water molecule can form hydrogen bonds with approximately two DMF molecules. Once the DMF molecules are saturated by water molecules, further addition of water breaks the formal structures and each water molecule can form only one or two hydrogen bonds with DMF[57]. When the water content is higher than 5%, DMF is slowly diluted and the exothermal effect fades gradually. Figures 6B, 6D and 6F showed the accumulated ΔH_{mix} as a function of WC. It is obvious that the micellization process during the titration can be divided into two stages. In stage I, at the beginning of water addition, the hydrophilic parts of the polyphosphazenes dissolve in water and the hydrophobic parts tend to aggregate to form micelles, which is supported by a strong exothermal effect. Once the micelles are formed, the hydrophobic core undergoes dehydration to maintain its mobility for morphological transitions at stage II, during which the process shows a strong endothermic nature. It should be noted that for PGOP-3 the endothermal effect in stage II was small due to the relatively low hydrophobic proportion. CWC values obtained by extrapolation between the two stages were 2.12% for PGOP-1, 3.38% for PGOP-2 and 5.15% for PGOP-3, which were similar to the results obtained by SLS.

Conclusion

In summary, poly(*β*-D-glucose-*Co*-1-octyl)phosphazenes with mutable hydrophilicity or hydrophobicity were synthesized via thiol-ene click reactions, in which all of the allyl groups of the precursor PBAAP were converted into glucose and octyl moieties. Consequently, PGOP-1,

PGOP-2 and PGOP-3 with different degrees of functionalization were obtained. This type of random copolymer self-assembled in both water and DMF-water mixed solvents. In water, PGOP-1, PGOP-2 and PGOP-3 formed micelles with broad size distributions (PDI=0.42-0.73). In DMF-water mixed solvents, consecutive morphological transitions from micelles through rods and finally to vesicles with increasing water content (WC) were observed. PGOP-1, the most hydrophobic polymer, had the lowest critical water content (CWC) and the fastest morphological transition as observed by Static Light Scattering (SLS) and Transmission Electron Microscopy (TEM). Size expansion of the self-assemblies during water addition was also observed by Dynamic Light Scattering (DLS). As measured by Isothermal Titration Calorimetry (ITC), the process of micellization varied from exothermic to endothermic with increasing water content. Similar CWC values to those determined by SLS were also obtained by ITC. We believe that through careful molecular design of random polyphosphazenes, controllable and versatile organized nanostructures can be obtained.

Acknowledgement

The authors would like to thank the financial support from the National Natural Science Foundation of China (Grant No. 21274126 and No.51473143).

References

[1] L. Zhang and A. Eisenberg, *Science*, 1995, **268**, 1728-1731.

[2] L. Zhang and A. *Eisenberg, Polym. Adv. Technol.*, 1998, **9**, 677-699.

[3] A. V. Kabanov, T. K. Bronich, V. A. Kabanov and K. Yu, A. Eisenberg, *J. Am. Chem. Soc.*, 1998, **120**, 9941-9942.

[4] D. E. Discher and A. Eisenberg, *Science*, 2002, **297**, 967-973.

[5] T. Stephan, S. Muth and M. Schmidt, *Macromolecules*, 2002, **35**, 9857-9860.

[6] E. Hoppenbrouwers, Z. Li and G. Liu, *Macromolecules*, 2003, **36**, 876-881.

[7] H. J. Dou, M. Jiang, H. S. Peng, D. Y. Chen and Y. Hong, *Angew. Chem. Int. Ed.*, 2003, **42**, 1516-1519.

[8] C. L. McCormick, A. B. Lowe and N. Ayres, *Encyclopedia of Polymer Science and Technology*, 2004, **12**, 452-521.

[9] L. Zhang and A. Eisenberg, *Macromolecules*, 1996, **29**, 8805-8815.

[10] H. Shen, L. Zhang and A. Eisenberg, *J. Phys. Chem. B*, 1997, **101**, 4697-4708.

[11] Y. Yu, L. Zhang and A. Eisenberg, Macromolecules, 1998, **31**, 1144-1154.

[12] A. Choucair and A. Eisenberg, *Eur. Phys. J. E.*, 2003, **10**, 37-44.

[13] Y. Zhao, F. Sakai , L. Su, Y. Liu, K. Wei, G. Chen and M. Jiang, *Adva. Mater.*, 2013, **25**, 5215-5256.

[14] C. Price, *Pure Appl. Chem.*, 1983, **55**, 1563-1572.

[15] J. S. Pedersen and C. Svaneborg, *Curr. Opin. Colloid Interface Sci.*, 2002, **7**, 158-166.

[16] H. Shen and A. Eisenberg, *Angew. Chem. Int. Ed.*, 2000, **39**, 3310-3312.

[17] E. B. Zhulina and O. V. Borisov, *Macromoleculaes*, 2002, **35**, 9191-9203.

[18] K. Kataoka, A. Harada and Y. Nagasaki, *Adv. Drug Deliv. Rev.*, 2001, **47**, 113-131.

[19] A. Eisenberg, *Chem. Mater.*, 1998, **10**, 1021-2028.

[20] X. Liu, J. S. Kim, J. Wu and A. Eisenberg, *Macromolecules*, 2005, **38**, 6749-6751.

[21] P. L. Soo and A. Eisenberg, *J. Polym. Sci. Part B: Polym. Phys.*, 2004, **42**, 923-938.

[22] F. Tian, Y. Yu, C. Wang and S. Yang, *Macromolecules*, 2008, **41**, 3385-3388.

[23] X. Zhu and M. Liu, *Langmuir*, 2011, **27**, 12844-12850.

[24] K. Salimi, Z. M.O. Rzayev and E. Pişkin, *Appl. Clay Sci.*, 2014, **101**, 106-118.

[25] K. Kaushlendra and S. K. Asha, *Langmuir*, 2012, **28**, 12731-12743.

[26] N. T. D. Tran, Z. Jia, N. P. Truong, M. A. Cooper and M. J. Monteiro, *Biomacromolecules*, 2013, **14**, 3463-3471.

[27] F. Sakai, G. Chen and M. Jiang, *Polym. Chem.*, 2012, **3**, 954-961.

[28] A. Besheer, J. Vogel, D. Glanz, J. Kressler, T. Groth and K. Mader, *Mol. Pharm.*, 2009, **6**, 407-415.

[29] A. Mahdavi, L. Ferreira, C. Sundback, J. W. Nichol, E. P. Chan, D. J. D. Carter, C. J. Bettinger, S. Patanavanich, L. Chignozha, E. B. Joseph, A. Galakatos, H. Pryor, I. Pomerantseva, P. T. Masiakos, W. Faquin, A. Zumbuehl, S. Hong, J. Borenstein, J. Vacanti, R. Langer and J. M. Karp, *Proc. Natl. Acad. Sci. U. S. A.*, 2008, **105**, 2307-2312.

[30] C. Bettinger, J. Bruggeman, J. Borenstein and R. Langer, *Biomaterials*, 2008, **29**, 2315-2325.

[31] D. Nguyen, J. Green, J. Chan, D. Anderson and R. Langer, *Adv. Mater.*, 2008, **20**, 1-12.

[32] H.R. Allcock and R.L. Kugel, *J. Am. Chem. Soc.*, 1965, **87**, 4216.

[33] H.R. Allcock, R.L. Kugel and K. Valan, *J. Inorg. Chem.*, 1966, **5**, 1709-1715.

[34] H. R. Allcock, *Appl. Organometal. Chem.*, 1998, **12**, 659-666.

[35] H.R. Allcock and A.G. Scopelianos, *Macromolecules*, 1983, **16**, 715-719.

[36] H.R. Allcock and S.R. Pucher, *Macromolecules*, 1991, **24**, 23-34.

[37] M.J. Kade, D.J. Burke and C.J. Hawker, *J. Polym. Sci. part A: Polym. Chem.*, 2010, **48**, 743-750.

[38] Y.C. Qian, X.J. Huang, C. Chen, N. Ren, X. Huang and Z.K. Xu, *J. Polym. Sci. part A: Polym. Chem.*, 2012, **50**, 5170-5176.

[39] H. R. Allcock and N. L. Morozowich, *Polym. Chem.*, 2012, **3**, 578-590.

[40] C. T. Laurencin, M. E. Norman, H. M. Elgendy, S. F. El-Amin, H. R. Allcock, S. R. Pucher and A. A. Ambrosio, *J. Biomed. Mater. Res.*, 1993, **27**, 963-973.

[41] H. R. Allcock, P. E. Austin and T. X. Neenan, *Macromolecules*, 1982, **15**, 689-693.

[42] C. T. Laurencin, H. J. Koh, T. X. Neenan, H. R. Allcock and R. Langer, *J. Biomed. Mater. Res.*, 1987, **21**, 1231-1246.

[43] S. M. Ibim, S. F. El-Amin, M. E. Goad, A. M. Ambrosio, H. R. Allcock and C. T. Laurencin, *Pharm. Dev. Technol.*, 1998, **3**, 55-62.

[44] M. Deng, S. G. Kumbar, Y. Wan, U. S. Toti, H. R. Allcock and C. T. Laurencin, *Soft Matter*, 2010, **6**, 3119-3132.

[45] M. Heyde, M. Claeyssens and E. H. Schacht, *Biomacromolecules*, 2008, **9**, 672-677.

[46] Y. X. Yang, Z. W. Zhang, L. L. Chen, W. W. Gu and Y. P. Li, *Biomacromolecules*, 2010, **11**, 927-933.

[47] J. Zhang, L. Qiu, X. Li, Y. Jin and K. Zhu, *Small*, 2007, **3**, 2081-2093.

[48] I. Teasdale and O. Brüggemann, *Polymers*, 2013, **5**, 161-187.

[49] C. Zheng, X. Yao and L. Qiu, *Macromol. Biosci.*, 2011, **11**, 338-343.

[50] Z. C. Tian, C. Chen and H. R. Allcock, *Macromolecules*, 2014, **47**, 1065-1072.

[51] N. Ren, X. J. Huang, X. Huang, Y. C. Qian, C. Wang and Z. K. Xu, *J. Polym. Sci. part A: Polym. Chem.*, 2012, **50**, 3149-3157.

[52] C. Chen, X. J. Huang, Y. Liu, Y. C. Qian and Z. K. Xu, *Polymer*, 2014, **55**, 833-839.

[53] M.F. Francis, M. Cristea and F.M. Winnik, *Pure Appl. Chem.*, 2004, **76**, 1321-1335.

[54] R. Ma and L. Shi, *Polym. Chem.*, 2014, **5**, 1503-1518.

[55] K. Wei, L. Li,a S. X. Zheng, G. Wang and Q. Liang, *Soft Matter*, 2014, **10**, 383-394.

[56] M. Shokouhi, A. H. Jalili, M. H. Jenab and M. Vahidi, *J. Mol. Liq.*, 2013, **186**, 142-146.

[57] W. Feng and G. Z. Jia, *Physica A*, 2014, **404**, 315-322.

Figure Captions

Scheme 1. Morphological transition of poly(*β*-D-glucose-*co*-1-octyl)-phosphazene in DMF/H_2O mixture.

Scheme 2. Synthesis of poly(*β*-D-glucose-*co*-1-octyl)phosphazene via a two-step thiol-ene coupling.

Table 1. Parameters for synthesis of poly(*β*-D-glucose-*co*-1-octyl) -phosphazene with different hydrophilic/hydrophobic ratios.

Figure 1. ^{1}H NMR for poly(*β*-D-glucose-*co*-1-octyl)phosphazenes.

Figure 2. Mean diameter of PGOP-1, PGOP-2 and PGOP-3 in aqueous solution (0.5mg/mL).

Figure 3. TEM images of PGOP-1 (a,b), PGOP-2 (c,d) and PGOP-3 (e,f) in aqueous solution (0.5mg/mL).

Figure 4. Light scattering intensity in function of water content for PGOP-1, PGOP-2 and PGOP-3 in DMF/water mixed solution. The morphologies corresponding to the dots in the circles were viewed by TEM (see Table 2)

Table 2. TEM images of self-assembles at different water content for PGOP-1, PGOP-2 and PGOP-3.

Figure 5. Mean diameter of PGOP-1, PGOP-2 and PGOP-3 in DMF-water mixed solution (0.2mg/mL).

Figure 6. Observed heat of each injection of water into PGOP-1, PGOP-2 and PGOP-3 (0.2mg/mL) in DMF (a, c and e) and accumulated heat in function of water content during titration process (b, d and f).

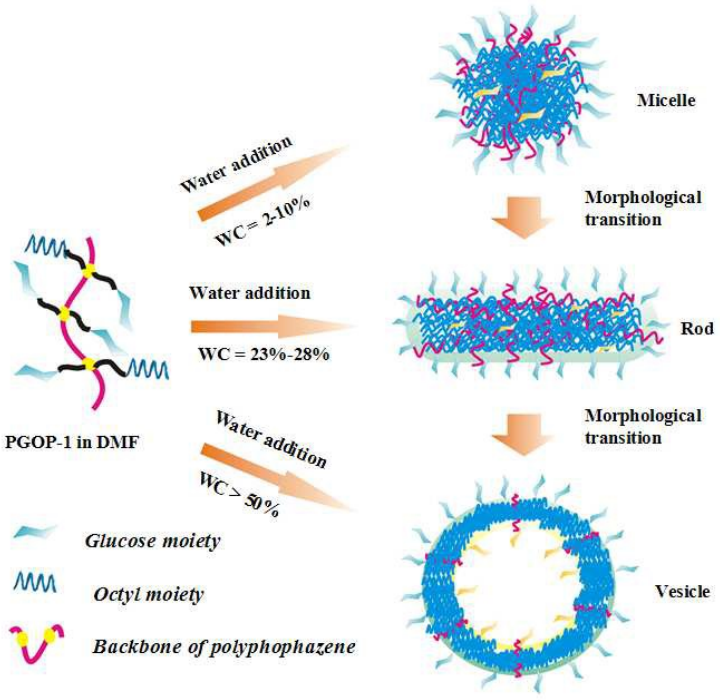

Scheme 1. Morphological transition of poly(*β*-D-glucose-*co*-1-octyl)-phosphazene in DMF/H_2O mixture.

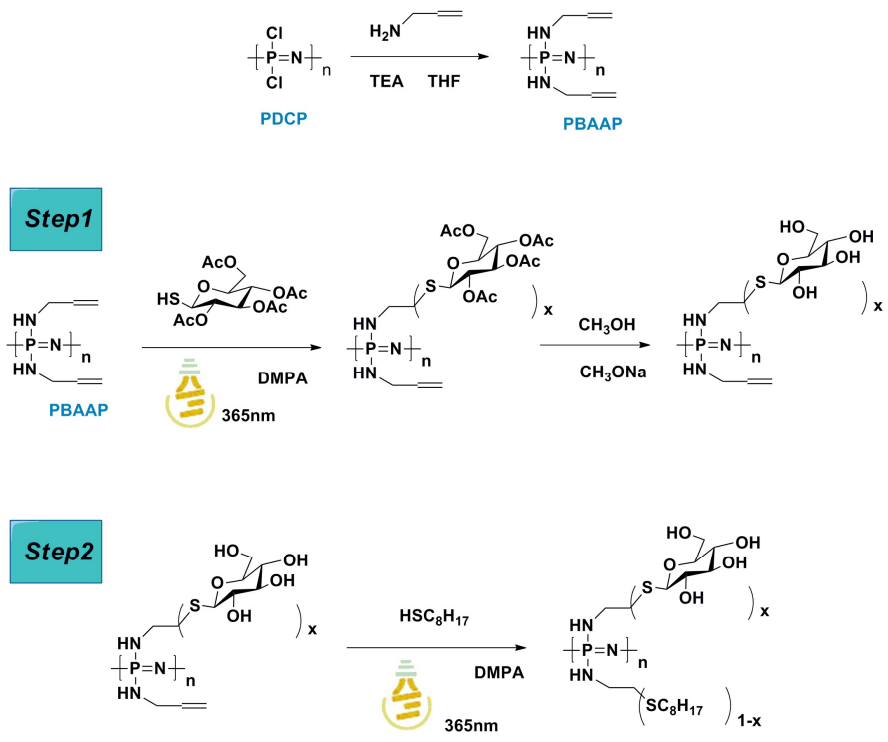

Scheme 2. Synthesis of poly(*β*-D-glucose-*co*-1-octyl)phosphazene via a two-step thiol-ene coupling.

Table 1. Parameters for synthesis of poly(*β*-D-glucose-*co*-1-octyl) -phosphazene with different hydrophilic/hydrophobic ratios.

Sample name	First step reaction time (min)	Glucosylation degree	Mn (g/mol)	Mw (g/mol)	PDI
PGOP-1	40	58.1%	2.37×10^4	3.68×10^4	1.55
PGOP-2	120	74.1%	2.46×10^4	4.02×10^4	1.63
PGOP-3	240	87.0%	2.53×10^4	3.89×10^4	1.54

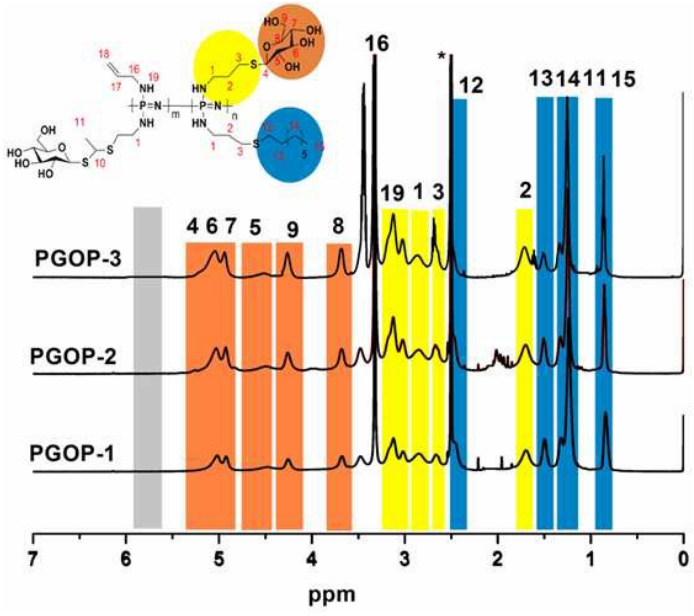

Figure 1. ^{1}H NMR for poly(*β*-D-glucose-*co*-1-octyl)phosphazenes.

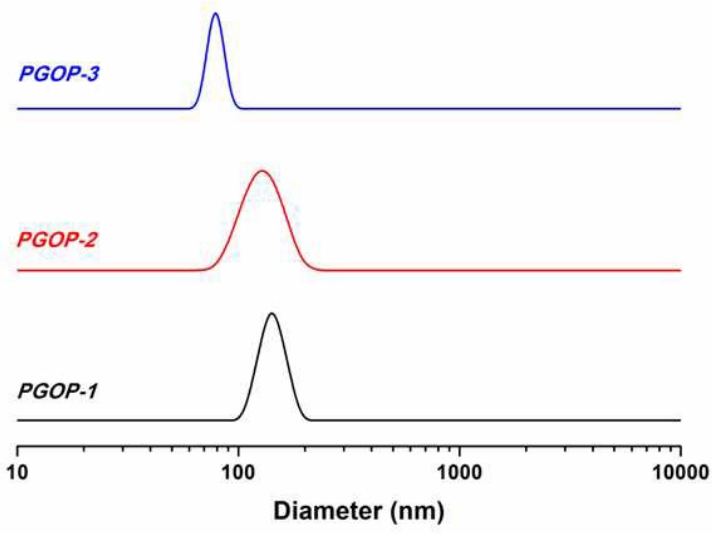

Figure 2. Mean diameter of PGOP-1, PGOP-2 and PGOP-3 in aqueous solution (0.5mg/mL).

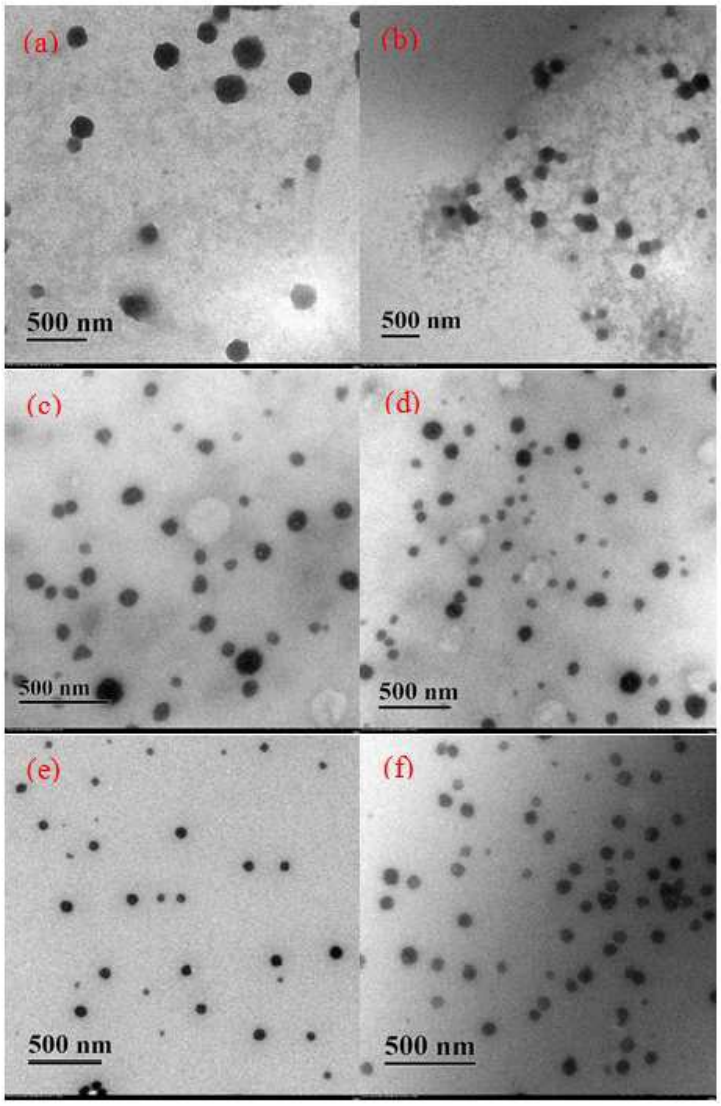

Figure 3. TEM images of PGOP-1 (a,b), PGOP-2 (c,d) and PGOP-3 (e,f) in aqueous solution (0.5mg/mL).

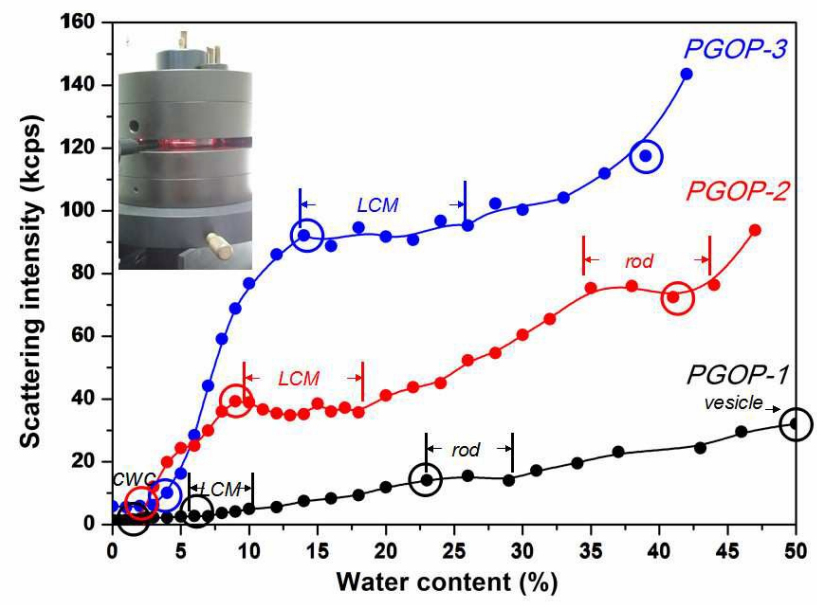

Figure 4. Light scattering intensity in function of water content for PGOP-1, PGOP-2 and PGOP-3 in DMF/water mixed solution. The morphologies corresponding to the dots in the circles were viewed by TEM (see Table 2).

Table 2. TEM images of self-assembles at different water content for PGOP-1, PGOP-2 and PGOP-3.

Morphology	PGOP-1	PGOP-2	PGOP-3
Micelles @ CWC	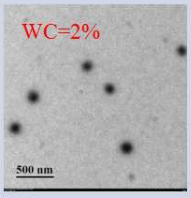	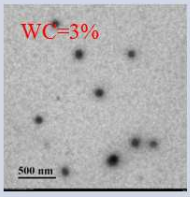	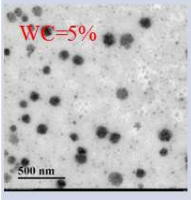
LCM	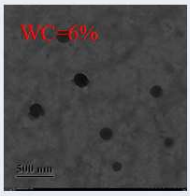	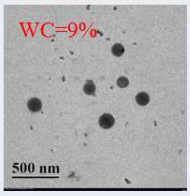	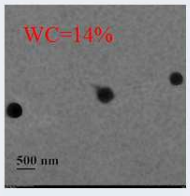
Rod	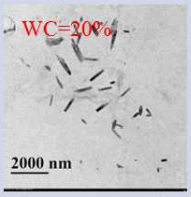	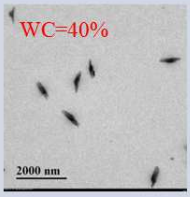	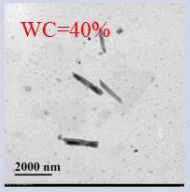
Vesicle	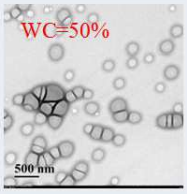		

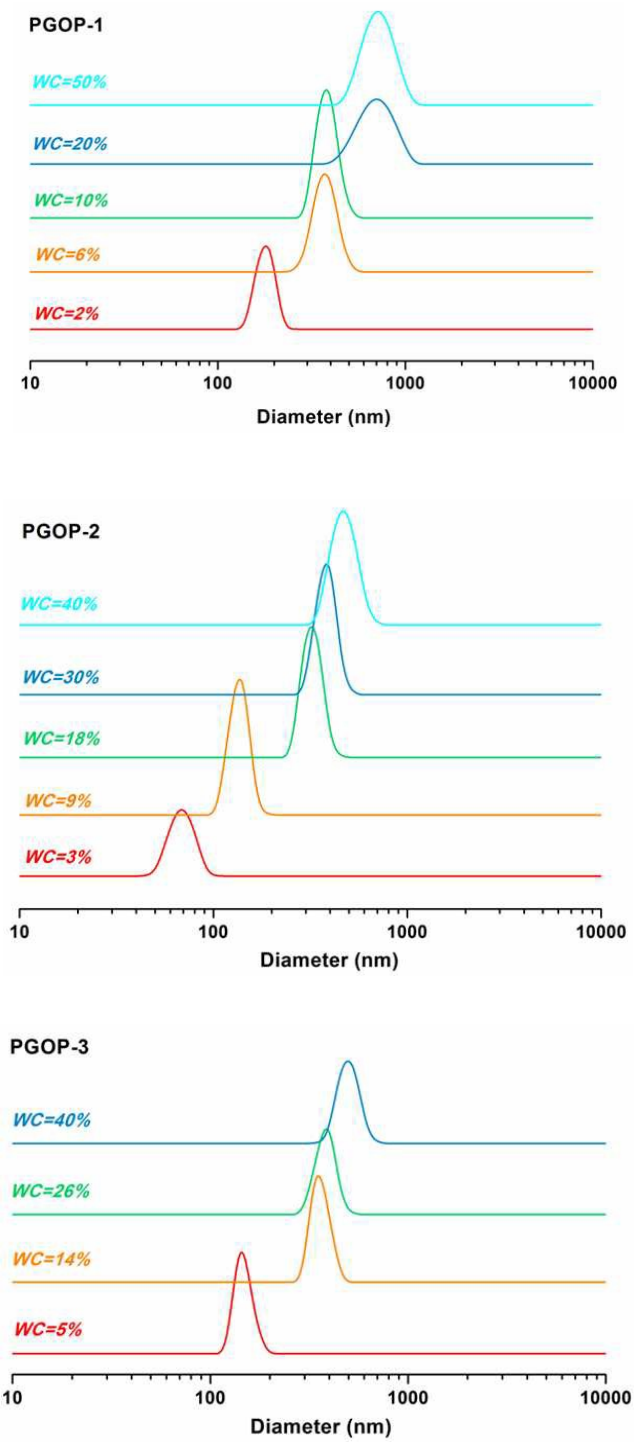

Figure 5. Mean diameter of PGOP-1, PGOP-2 and PGOP-3 in DMF-water mixed solution (0.2mg/mL).

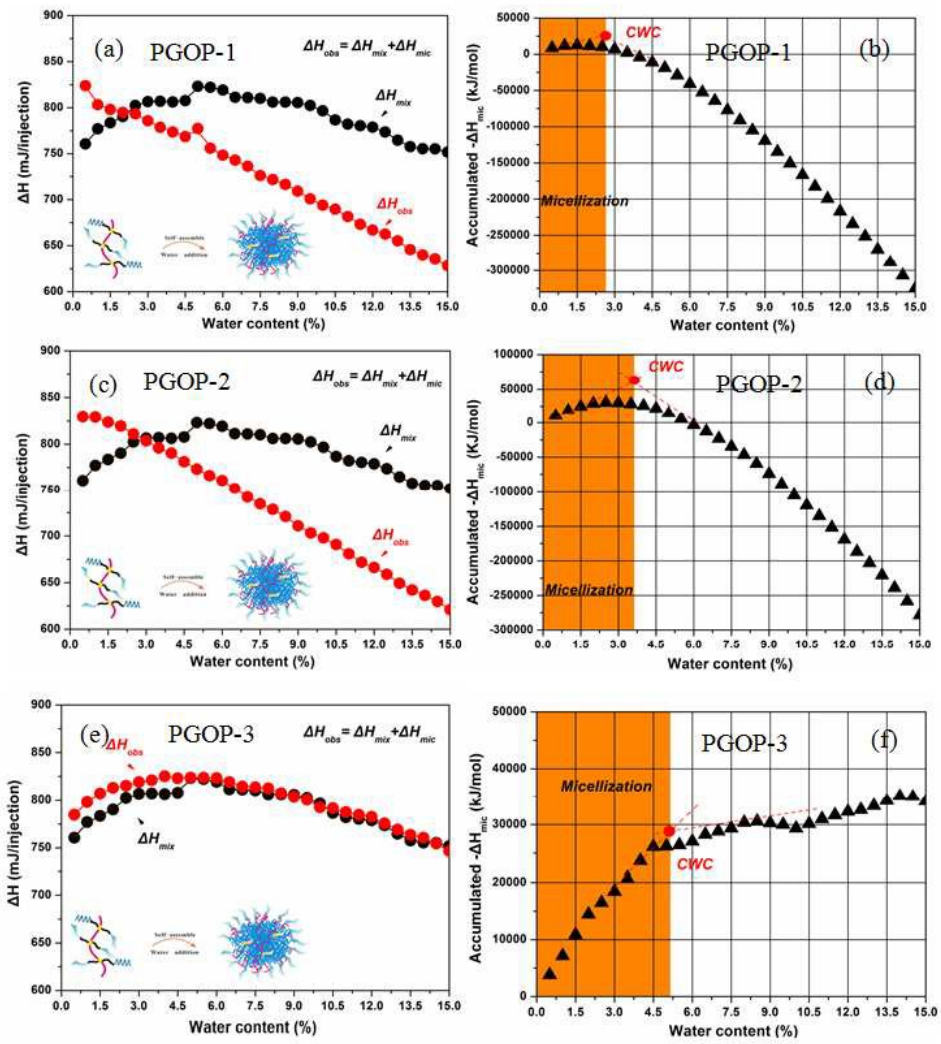

Figure 6. Observed heat of each injection of water into PGOP-1, PGOP-2 and PGOP-3 (0.2mg/mL) in DMF (a, c and e) and accumulated heat in function of water content during titration process (b, d and f).

Supporting Information

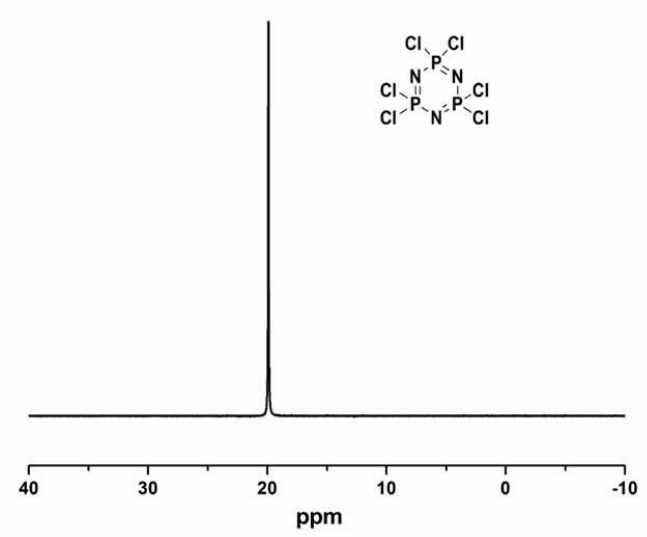

Figure S1 ^{31}P NMR of hexachlorocyclophosphazene (HCCP).

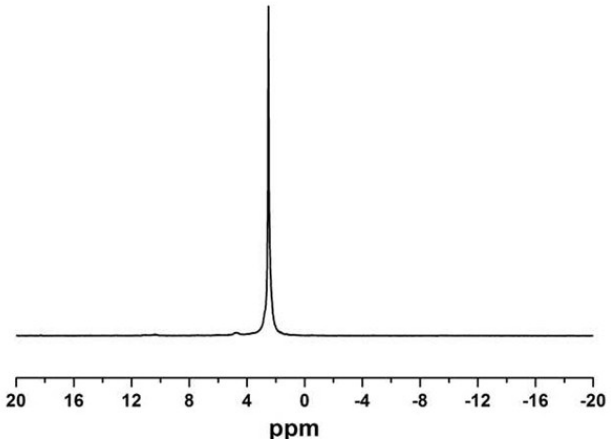

Figure S2. ^{31}P NMR for poly[bis(allylamino)phosphazene] (PBAAP).

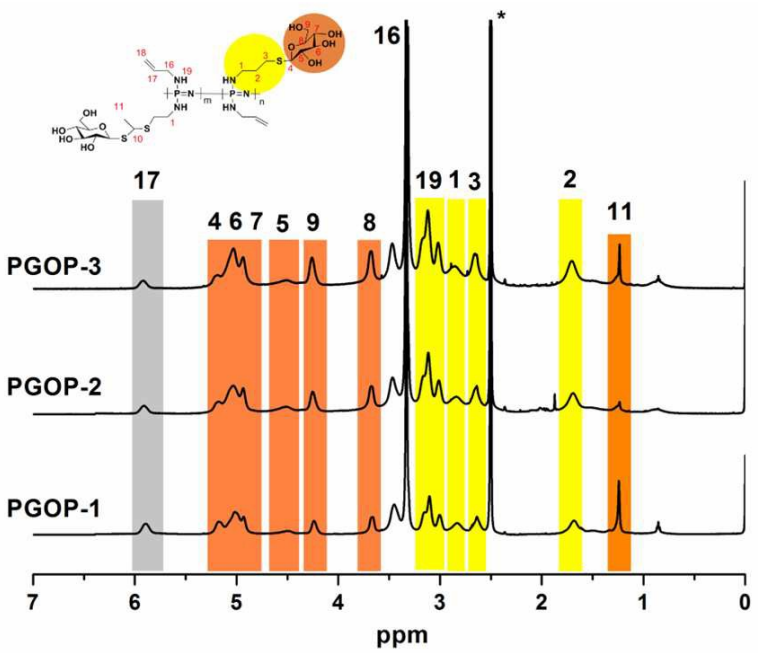

Figure S3. ^{1}H NMR for glycosylated polyphosphazene.

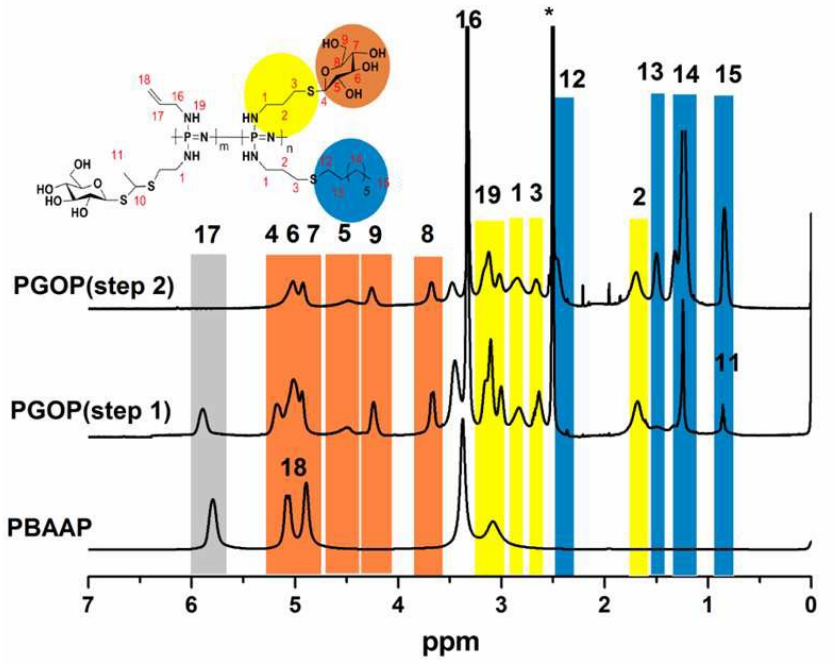

Figure S4 ^{1}H NMR for PBAAP, PGOP-1 after first step click reaction and PGOP-1 after second step click reaction.

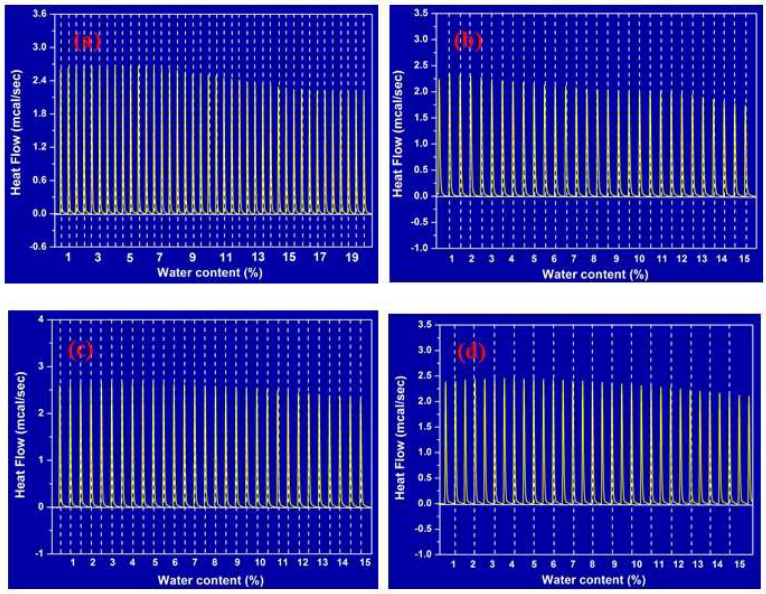

Figure S5. Titration heat flow of water-DMF (a), water-PGOP-1 (0.2 mg/mL) in DMF (b); water-PGOP-2 (0.2 mg/mL) in DMF (c) and water-PGOP-3 (d). The water was slowly injected into DMF solution at the rate of 0.05 wt%/s. The volume of water per injection was 0.5 wt%.

Table of Content

Self-assembly and Morphological Transitions of Random Amphiphilic Poly(*β*-D-glucose-*Co*-1-octyl) phosphazenes

Chen Chen; Yue-Cheng Qian; Chuan-bin Sun; Xiao-Jun Huang

A new kind random copolymer, poly(*β*-D-glucose-*Co*-1-octyl)phosphazene (PGOP), can self-assemble and regulate itself to form different morphologies in aqueous solution and water-DMF mixed solution. Variation in the proportion of hydrophilic/hydrophobic moieties on the phosphazene backbone leads to different morphological transition rates and thermodynamics for micellization.

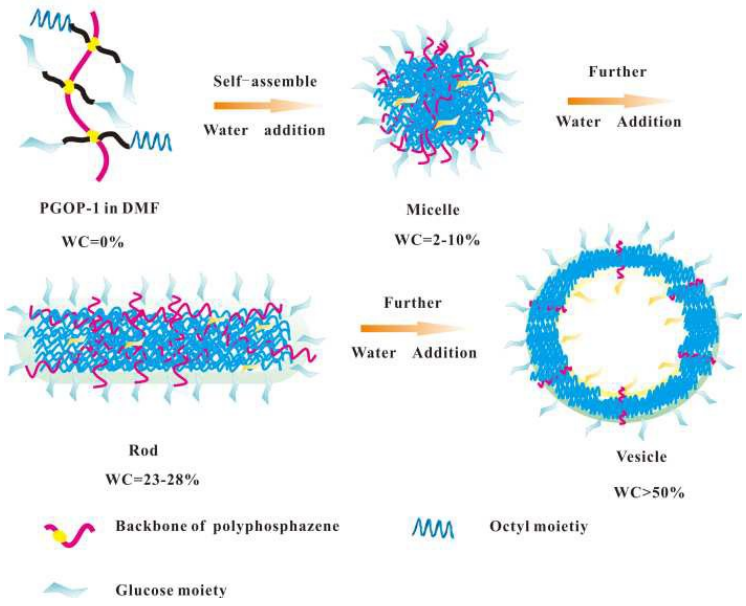

Table of contents